Analysis of Microstructure of Silicon Carbide Fiber by Raman Spectroscopy

Baohong JIN and Nanlin SHI†
Institute of Metal Research, Chinese Academy of Sciences, Shenyang 110016, China
[Manuscript received June 9, 2007, in revised form January 2, 2008]

The SiC fiber was prepared by chemical vapour depostion, which consists of tungsten core, SiC layer and carbon coating. The microstructure of the fiber was investigated using Raman spectroscopy, illustrating SiC variation in different region of the fiber. The result shows that the SiC layer can be subdivided into two parts in the morphologies of SiC grains; their sizes increase and their orientations become order with increasing distance from the fiber center. It is demonstrated that the mount of free carbon in the fiber is responsible for the variation of SiC grains in sizes and morphologies. The analysis of Raman spectra shows that the predominant β-SiC has extensive stacking faults within the crystallites and mixes other polytypes and amorphous SiC into the structure in the fiber.

KEY WORDS: Raman spectra; Optical phonon; SiC fiber; Carbon content

1. Introduction

Silicon carbide (SiC) fibers prepared by chemical vapour deposition (CVD) have been widely used for their high strength, corrosion resistance and exceptional high temperature stability. Since the small changes in the microstructure of SiC fiber will affect its mechanical strength[1], it is very important to study the microstructure of the fiber. In recent years, the CVD SiC fibers with carbon-rich has been studied in the Institute of Metal Research, Chinese Academy of Sciences. It is found that the excess carbon plays an important role in improving tensile strength of the SiC fiber, which is quite different from other fibers in their microstructure. There is few report on the SiC fibers with carbon-rich, therefore the purpose of this paper is to investigate the microstructure of the fiber using Raman spectroscopy, which can distinguish the crystallization states of SiC and variation in different region, as well as carbon content in the fiber.

2. Experimental

The SiC fiber used in this experiment was fabricated by CVD. SiC was deposited onto a continuous tungsten (W) wire. An outer carbon coating was also deposited by CVD on the surface of this fiber to protect it. In addition, the carbon-rich in the fiber was obtained by regulating the condition of the CVD process. The Raman spectra studies were carried out on a LabramHR800 Raman Microscope, using the 632.8 nm line of He-Ne laser as the excitation source, and the laser spot on the sample was focused to a 2 μm-diam spot size with an optical microscope. The examination was performed simply on polished cross-section of these SiC fibers, and then the different Raman bands of the selected points (from A to F) which are taken from the center to the surface of the fiber were obtained by moving the sample in intervals of about 5 μm (as shown in Fig.1). Such Raman spectra can give visual variation of SiC bands with the distance from fiber center.

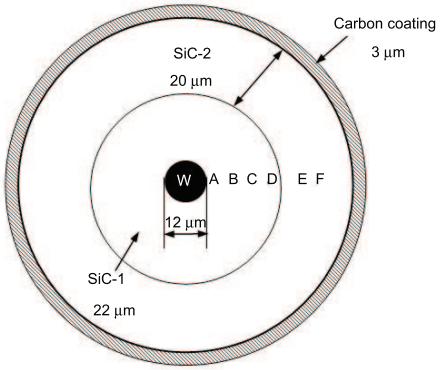

Fig.1 Schematic drawing of the SiC fiber microstructure

3. Results and Discussion

3.1 SEM image of the fiber

The cross-sectional scanning electron microscope (SEM) micrograph of the fiber is given in Fig.2. It can be observed that this fiber consists of three parts: W core about 12 μm in diameter, SiC layer with nearly 42 μm in thickness, and carbon coating with nearly 3 μm in thickness. The SiC layer extends radially, which can be subdivided into two sublayers in the morphologies of the SiC grains, *i.e.*, SiC-1 (about 22 μm in thickness) and SiC-2 about 22 μm in thickness) sublayers (as shown in Figs.1 and 2). Figure 3(a) shows that the SiC grains in the inner part (SiC-1 layer) are very small with random orientation. From Fig.3(b), it is noticed that there is an obviously interface between the SiC-1 and SiC-2 sublayers, which will be discussed in the latter. However the sizes and morphologies of the SiC grains in SiC-2 sublayer are quite different from those of the SiC grains in SiC-1

† Prof., to whom correspondence should be addressed,
E-mail: nlshi@imr.ac.cn.

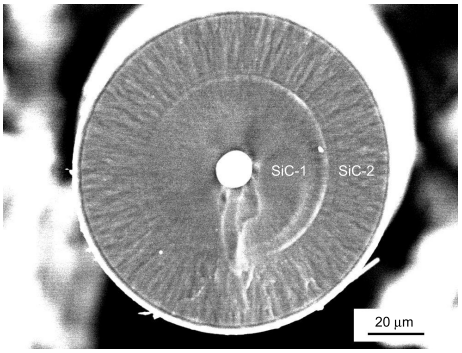

Fig.2 Cross-sectional SEM micrograph of the SiC fiber

sublayer. The elongated columnar SiC grains in the outer part (SiC-2 layer) can be seen distinctly and their directions are finely parallel to the fiber radius, as shown in Fig.3(c). On the whole, the SiC grains become larger and their directions become order gradually with increasing distance from W core. The carbon coating on the surface of the fiber can also be clearly observed.

3.2 X-ray diffraction observations

The X-ray diffraction (XRD) pattern has been obtained from the powders of the fiber in order to understand the SiC crystallites and their directions. As shown in Fig.4, there are three main peaks (111), (220), (311) referring to β-SiC crystallites, and the peak (111) is the strongest in the all, suggesting that the main constituent of the fiber is β-SiC crystallites with the main plane (111)[2]. In addition, the peaks at 26.6° and 50.1° (2θ value) are due to the graphite crystallites. Some weak peaks from W can be also found in the XRD pattern.

3.3 Analysis of SiC

The Raman spectra from the inner part to surface of the fiber are presented in Fig.5(a–c). It is reported that SiC gives Raman scattering from a transverse optic (TO) phonon at approximately 790 cm^{-1} and a longitudinal optic phonon (LO) at 973 cm^{-1}[3]. In this work, the TO and LO peaks of SiC crystallites in different regions of the fiber have been investigated, however the observed TO and LO peak positions are not in good agreement with those of the report. Figure 5(a) displays Raman bands in SiC-1 layer, which were taken from A and B selected points (about 15 and 20 μm distance from the fiber center, respectively). From these bands, it can be observed that two distinct TO and LO peaks of SiC at about 775 and 920 cm^{-1} are both quite broad and in low intensities. These scattering would be forbidden in large, perfect single crystals[3,4]. Thus it can be regarded as SiC remaining poorly crystallization, small crystal size and amorphous SiC in inner part of the fiber. The 790 cm^{-1} phonon shifts down to 775 cm^{-1}, and the 973 cm^{-1} shifts down to 920 cm^{-1}, which are probably due to the small crystallites[4]. The TO and LO peak positions of the SiC crystallites indicate that the predominant SiC polytype is β-SiC in this fiber[5]. Since the Raman scattering efficiency of SiC is much lower than that of carbon[6], and in combination with the small grain sizes in this region, the SiC peaks would be very weak.

Figure 5(b) shows the Raman bands which were taken from C and D selected points (about 24 and 28 μm distance from the fiber center, respectively). In these bands, the TO and LO peaks of SiC become narrower and stronger than those of the bands from A and B selected points, which are attributed to the result that SiC crystallites become larger and perfect with increasing distance from the fiber center. In case of the above bands, since the LO peaks are broad and asymmetric, it is hard to identify the precise peak position, implying the presence of amorphous SiC or other SiC polytypes in the SiC-1 layer. The appearance of the overlapping SiC bands is also due to the extensive stacking faults in SiC crystallites. Figure 5(c) presents the Raman bands in outer part (SiC-2 layer) of the fiber, which were taken from E and F selected points (about 35 and 40 μm distance from the fiber center, respectively). Seen from these bands, the TO and LO peaks of SiC are quite sharp and intense, which appear at about 778 and 889 cm^{-1}, confirming that the SiC crystallites are very perfect and larger in this region.

For the all SiC bands, it can be observed that the TO and LO peaks of SiC become more and more narrow and strong with increasing fiber radius. Then the conclusion can be drawn that the SiC crystallites increase in crystal size and perfection by moving out towards the fibre surface, which is consistent with previous SEM studies. On the other hand, the peaks of SiC crystallite shifts down to low wavenumbers, implying that SiC crystallites are suffered from heavy tensile stresses[7,8]. We believe that the intensity variation of the SiC bands is correlated to the SiC grain size and crystallization in different parts of the fiber.

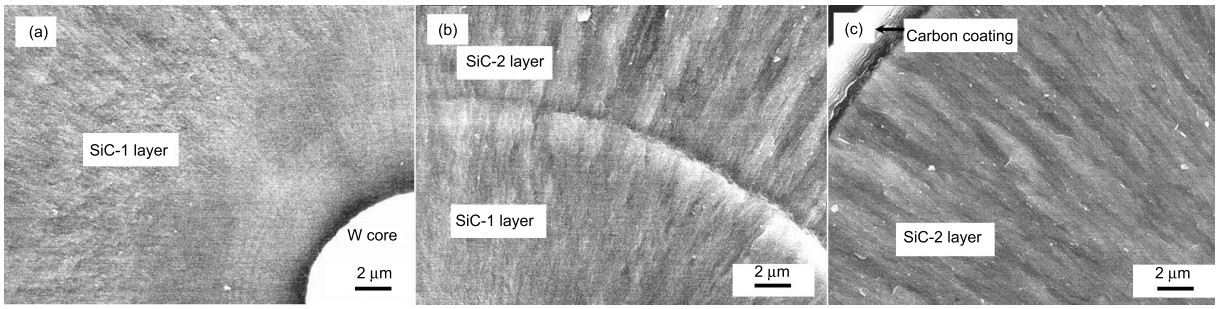

Fig.3 Cross-sectional SEM micrographs taken from the inner to the outer region of the fiber (a) from SiC-1 layer (b) from interface between SiC-1 and SiC-2 layers (c) from SiC-2 layer

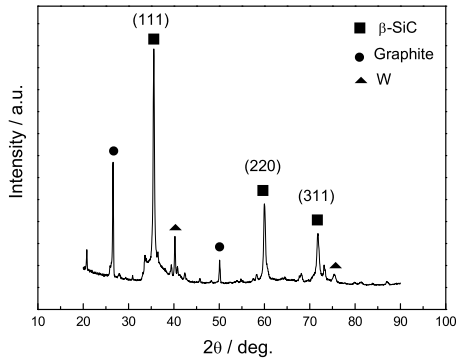

Fig.4 XRD pattern from SiC powders of the fiber

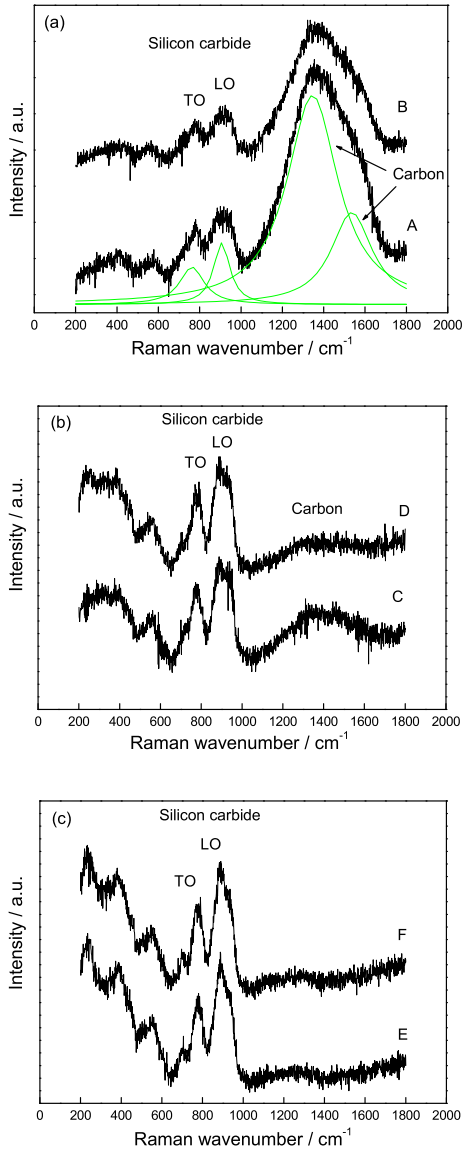

Fig.5 Raman spectra obtained from the inner to outer region of the fiber: (a), (b) from SiC-1 sublayer, and the A , B, C and D points at 15, 20, 24 and 28 μm distance from the fiber center, respectively (c) from SiC-2 sublayer, and the E and F points at 35 and 40 μm distance away from the fiber center, respectively

In addition, all Raman bands in the range of 200–600 cm^{-1} appear to be some of small peaks, arising from the SiC acoustic phonons. However, the presence of phonon scattering mixes phonons with difference wavevectors[5,9]. The hexagonal or orthorhombic polytype weaker bands from folded transverse acoustic (TA) modes would be observed in this range, but their bands from folded TO modes would appear in the range of 700–1000 cm^{-1}[10]. As shown in Fig.5(b) and (c), some small peaks appear at around 237 and 380 cm^{-1}, in combination with the small peak appearing at 705 cm^{-1}, therefore it can be assumed to be the presence of α-SiC (polytype 6H)[6,10]. Moreover the Raman bands of α-SiC become narrow and strong toward the surface of the fiber, due to the increase in crystal size and perfection of α-SiC crystallites. In a summary, the predominant β-SiC crystallites with extensive stacking faults mix other polytypes and amorphous SiC into the structure of the SiC fiber.

3.4 Free carbon in the fiber

The microstructure of the SiC fiber used in this work is attributed to the free carbon content in the SiC layer when compared to other fibers. As shown in Fig.5(a), the carbon bands exhibit an overlapping peak in the range of 1000–1800 cm^{-1}. In fact, it can be separated into two peaks, *i.e.*, 1343 and 1535 cm^{-1}, which correspond to the D and G peaks of crystalline graphite, respectively. Moreover the intensity ratio of the two peaks is a good measure of the crystallite size in the α-plane[11,12]. The D peak cannot appear in the spectrum of single crystal graphite[13,14], which results from the disorder of carbon crystals[15]. It means that there are mixtures of polycrystalline graphite and amorphous carbon in the SiC-1 layer. The intensity of the carbon bands decreases with increasing radius away from W core, implying the variation of the carbon content. Following the outer SiC-1 layer, the carbon bands are too broad and weak to identify the precise peak position, which correspond to amorphous carbon or absence of the carbon content, as given in Fig.5(b). However the evidence of carbon bands abruptly disappear in the interface between the SiC-1 and SiC-2 layers, and then the carbon band cannot be found any more in Fig.5(c). The analysis of carbon bands shows that the SiC-1 layer contains carbon-rich, which gradually decreases toward outer part of the layer, however there is absence of carbon in the SiC-2 layer. Since the excess carbon acts as diffusion barriers inhibitting the growth of the SiC grains but holding them together[16], the SiC grains in the region with high carbon content are more small and poor than those in the region with low carbon content. The result indicates that the interface within SiC layer is caused by the different carbon content in each SiC layer.

3.5 Free silicon in the fiber

Raman spectra from Fig.5(a–c) exhibit that there is a sharp band at around 560 cm^{-1}, which is ascribed to the LO mode of silicon[17]. There are also strong broad bands with peaks just below 500 cm^{-1}, which could be due to the presence of amorphous silicon with a TO band at around 475 cm^{-1}. Therefore it is a very useful information to confirm the presence of free silicon in the SiC fiber. On the other hand, the peak of free silicon crystallite shifts to high wave number, indicating that the silicon crystallite is suffered from

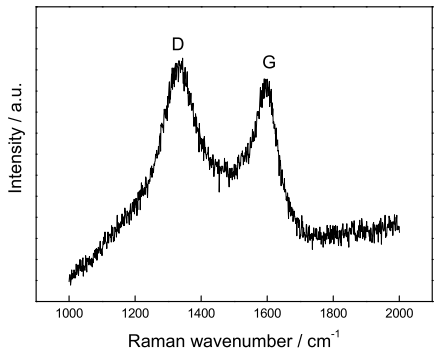

Fig.6 Raman spectra taken from carbon coating of the fiber

compressive stress[8] in the fiber.

3.6 Carbon coating

In Fig.6, there are two distinct carbon bands at around 1335.8 and 1596.5 cm^{-1} from the carbon coating, which correspond to the D band and G band of crystalline graphite, respectively[18]. The one at 1597 cm^{-1} has been assigned to the E_{2g} C-C (sp^2-bonded) stretching mode of single crystal graphite, the other at 1336 cm^{-1} is attributed to the A_{1g} C-C (sp^3-bonded) stretching mode and results from the crystal boundaries of polycrystalline graphite[19]. The results indicate that there are some graphitic crystals in carbon coating.

4. Conclusions

(1) β-SiC crystallites are predominant in SiC fiber, their sizes increasing and their orientations becoming parallel to the radial direction of the fiber with increasing the distance from fiber center.

(2) The SiC crystallites with extensive stacking faults mix other polytypes into the structure in the fiber.

(3) There are different carbon content in different SiC layer, and the interface within SiC layer is caused by the different carbon content in each SiC layer.

(4) The SiC grains in the region with high carbon content are more small and poor than those in the region with low carbon content.

Acknowledgement

The author thanks the Raman Spectroscopy Laboratory of Institute of Metal Research, Chinese Academy of Sciences for the support in the accomplishment of this paper.

REFERENCES

[1] Y.Ward, R.J.Young and R.A.Shatwell: *J. Mater. Sci.,* 2001, **36,** 59.
[2] V.V.Pujar and J.D.Cawley: *J. Am. Ceram. Soc.,* 1995, **78**(3), 775.
[3] D.W.Feldman, J.Parker, W.Choyke and L.Patrick: *Phys. Rev.,* 1968, **173,** 787.
[4] H.Richter, Z.P.Wang and L.Ley: *Solid State Commun.,* 1981, **39,** 625.
[5] H.Okumura, E.Sakuma, J.H.Lee, H.Mukaida, S.Yoshida and K.Endo: *J. Appl. Phys.,* 1987, **61,** 1134.
[6] Y.Sasaki, Y.Nishina, M.Sato and K.Okamura: *J. Mater. Sci.,* 1987, **22,** 443.
[7] G.Pezzotti: *J. Raman Spectrosc.,* 1999, **30,** 867.
[8] O.Nina and G.Yury: *Key Eng. Mater.,* 2002, **206,** 1025.
[9] M.H.Brodsky and M.Cardona: *J. Non-Cryst. Solids.,* 1978, **31,** 81.
[10] M.Giuseppe, B.Aldo, F.Luca and B.Leandro: *J. Am. Ceram. Soc.,* 2004, **87,** 653.
[11] B.S.Elman, M.Shayegan, M.S.Dresselhaus, H.Mauzurek and G.Dresselhaus: *Phys. Rev.,* 1982, **B25,** 4142.
[12] A.B.Fuertes and T.A.Centeno: *J. Chem. Phys.,* 2005, **15,** 1079.
[13] F.Tuinstra and J.L.Koenig: *J. Chem. Phys.,* 1970, **53,** 1126.
[14] R.O.Dillon and J.A.Woodllam: *Phys. Rev.,* 1984, **B29,** 3482.
[15] M.A.Tamor and W.C.Vassell: *J. Appl. Phys.,* 1994, **76,** 3823.
[16] X.J.Ning, P.Pirouz and S.C.Farmer: *J. Am. Ceram. Soc.,* 1993, **76,** 2033.
[17] J.Kim, S.Tlali, H.E.Jackson, J.E.Webb and R.N.Singh: *Appl. Phys. Lett.,* 1996, **16,** 2352.
[18] P.Lespade, R.Al-Jishi and M.S.Dresselhaus: *Carbon,* 1982, **20,** 427.
[19] D.S.Knight and W.B.White: *J. Mater. Res.,* 1989, **4,** 385.